Electric-field-induced strong mixing between *e*1-*hh*1 and *e*1-*hh*2 excitons in asymmetric double quantum wells

Dong Kwon Kim* and D. S. Citrin
School of Electrical and Computer Engineering, Georgia Institute of Technology, Atlanta, Georgia 30332-0250, USA
and Unité Mixte Internationale 2958 Georgia Tech–CNRS, Georgia Tech Lorraine, 2, rue Marconi, 57070 Metz, France
(Received 11 June 2007; published 10 September 2007)

We analyze the electric-field-dependent strong mixing of the two near band-edge ground-state excitons in asymmetric double quantum wells (ADQWs). This excitonic mixing is mainly attributed to the Coulomb interactions between subbands and the valence-subband nonparabolicity. The effect of mixing on the energy levels and oscillator strengths is obtained by a comparison of results including and excluding the Coulomb interaction between *different* subband pairs which appears in the off-diagonal matrix elements of the Hamiltonian in the calculation of exciton states. We find that a substantial portion of the oscillator strength of the *e*1-*hh*1 ground-state exciton is due to the *e*1-*hh*2 subband pair in a bias range of the anticrossing region between pairs of valence subbands. Results also show that excluding the excitonic mixing effect results in significant error in both the energies and the oscillator strengths of the excitons in an ADQW with a thick barrier (3 nm). Even in an ADQW with a fairly thin barrier (1.2 nm), the error in the oscillator strengths can be substantial, although the errors in the computed energies may be tolerable. Detailed analysis of $k_{\|}$-dependent Coulomb matrix elements and exciton expansion coefficients reveals that neglecting the off-diagonal elements in the exciton Hamiltonian diminishes the contribution of the $k_{\|}$-dependent subband envelopes around the anticrossing in $k_{\|}$ space to the corresponding excitons. Further, it is demonstrated that the application of almost-degenerate perturbation theory to the uncoupled excitons with the intention of accounting for this mixing effect is to be approached with caution.

DOI: 10.1103/PhysRevB.76.125305 PACS number(s): 78.67.De, 71.35.Cc

I. INTRODUCTION

The experimental observation of the quantum-confined Stark effect in single quantum wells (SQWs)[1,2] initiated a vast number of theoretical and experimental investigations of the electro-optical properties of quantum wells (QWs).[3–10] Extensive band-gap engineering demonstrated that coupled double QW (CDQW) structures could offer enhanced electro-optical properties, and thus has been a popular research topic to the present day.[11–22] CDQWs exhibit more complicated bias-dependent optical properties than those of SQWs, thus requiring a more careful consideration of effects frequently neglected for SQWs, such as the mixing of excitons originating in different subband pairs. (This should not be confused with the spatial extension of subband envelope wave functions from well to well in CDQWs that occurs regardless of the Coulombic mixing of the subband pairs or valence subband mixing.) The mixing of excitons is pronounced when the energy difference between the two adjacent excitons is smaller than the typical exciton binding energy, which occurs not only in fairly broad SQWs with weak confinements but also in CDQWs. Valence-band mixing (VBM) affects both the energy levels and the oscillator strengths of excitons through the nonparabolic energy (E) dispersions of the valence subbands and wave-vector ($k_{\|}$)-dependent overlap integrals between the electron and hole envelope functions, leading to increased accuracy of the theoretical estimates. A convenient way of including the $k_{\|}$ dependences and exciton mixing is via the momentum-space approach.[8–10]

Early theoretical studies on DQWs, however, did not take full account of VBM, although they included the mixing of excitons in various ways. Bauer and Ando[7] included only the nonparabolic E-$k_{\|}$ dispersions of single particles, i.e., electrons or holes, in their calculation, where the excitonic mixing was explicitly included through the off-diagonal matrix elements of the effective-mass Hamiltonian. Lee *et al.*[12] calculated excitonic spectra of ADQWs in electric fields without including the mixing of excitons and VBM and obtained the fundamental optical properties. Fox *et al.*[14] included the mixing between ground-state excitons in symmetric coupled quantum wells, where the mixing effects appeared in the exciton wave functions as the modifications of the unmixed single-particle subband wave functions. They also pointed out that the anticrossing bias field of the two ground-state excitons shifts from that of the corresponding band-to-band transitions due to the exchange of the exciton binding energies. Kamizato and Matsuura[13] applied almost-degenerate perturbation theory to the unmixed ground-state excitons to account for the mixing in DQWs. Dignam and Sipe[16] analyzed in detail the four exciton states *e*1-*hh*1, *e*1-*hh*2, *e*2-*hh*1, and *e*2-*hh*2 [*en* (*hhm*) refers to the quantized n (m)th conduction (valence) subband] in symmetric and asymmetric CQWs in a static electric field by employing the variational method and showed that inter- and intrawell transitions strongly mix the radial components of exciton states, which agreed with the results of Kamizato and Matsuura. In DQWs with thin coupling barriers, however, the unmixed exciton model was found to yield good agreement with the experimental results.[17] These studies in essence did not require a deeply rigorous treatment of VBM effects because most of the involved excitonic anticrossings were between electron subbands, i.e., between *e*1-*hh*1 and *e*2-*hh*1, where VBM does not play an important role.

Numerous studies have demonstrated that incorporating an asymmetric coupled DQW can yield better performance of QW Stark electro-optic modulators[18–20] and can lead, further, to the development of new functional devices[21,22] for practical applications. In ADQWs, utilizing the heavy-hole subband anticrossing ($e1$-$hh1$ and $e1$-$hh2$), however, can be advantageous: The effective mass of the heavy hole is in general much greater than that of electrons in type-I QWs, which leads to stronger confinement and thus requires thinner barrier thickness for the same degree of anticrossing effect. This, in turn, can increase the overall absorption efficiency per unit thickness of the device. In addition, the bias field required for the anticrossing of the excitons near the band edge is much smaller than that of electron anticrossings, which potentially reduces the operating bias of the device. However, a complete theoretical analysis of these effects has hitherto not been reported. This is important since marked discrepancies between theory and experiment may show up in the oscillator strengths whereas the exciton binding energies may be computed with adequate accuracy in an overly simplified model.

In this paper, we study theoretically the effect of strong mixing of $e1$-$hh1$ and $e1$-$hh2$ s-like excitons on the energy levels and oscillator strengths of excitons within the anticrossing bias range while including the VBM rigorously within a momentum-space approach.[8–10] The effect of mixing is appreciated in two ADQW structures having different degrees of coupling between the two wells through the coupling barrier (CB, thickness $\sim$1.2 and 3 nm) by including and excluding the off-diagonal Coulomb matrix elements (between the two different subband pairs) in the effective-mass Hamiltonian for excitons. The validity of the results obtained from these models is discussed in terms of the oscillator-strength sum rule (f-sum rule). We find that the f-sum rule breaks down in models that ignore exciton mixing, the reason for which is sought by analyzing the $k_\parallel$-dependent Coulomb matrix element and the corresponding expansion coefficients of the exciton wave function. Further, we show that applying almost-degenerate perturbation theory to the two unmixed ground-state excitons obtained from the two-subband model which includes VBM should be carried out with caution in analyzing the electric-field-dependent optical properties of ADQWs, a technique that has often been employed to account for the mixing of excitons.

II. THEORY

In this section, we review briefly the key equations that are employed for the analysis of the excitons and the corresponding oscillator strengths, which encompass the fundamental equations for the calculation of excitons, mixing of excitons, and the application of almost-degenerate perturbation.

A. Fundamentals of the exciton calculation

Within the framework of effective-mass theory, the exciton envelope function in a quasi-two-dimensional structure is expressed as a linear combination of the associated electron and hole eigenstates,

$$\Psi_{\alpha,\mathrm{env}} = \sum_{n,m} \sum_{\mathbf{k}_\parallel,\mathbf{q}_\parallel} F_{nm}^{\alpha}(\mathbf{k}_\parallel,\mathbf{q}_\parallel) e^{i(\mathbf{k}_\parallel\cdot\boldsymbol{\rho}_e+\mathbf{q}_\parallel\cdot\boldsymbol{\rho}_h)} f_n(z_e,\mathbf{k}_\parallel) \sum_{\nu} g_m^{\nu}(z_h,\mathbf{q}_\parallel), \tag{1}$$

where n (m) is subband index of the electron (hole), α is the index that labels the exciton states, $\mathbf{k}_\parallel$ ($\mathbf{q}_\parallel$) is the in-plane wave vector of the electron (hole), $\boldsymbol{\rho}_{e(h)}$ is the in-plane coordinate of the electron (hole), f_n (g_m^{ν}) is the envelope function along the growth direction $z_{e(h)}$ of the electron (hole with the spin component $\nu=\pm 1/2$ or $\pm 3/2$), and $F_{nm}^{\alpha}(\mathbf{k}_\parallel,\mathbf{q}_\parallel)$ is the expansion coefficients that represent the contribution of the subband pairs to the exciton state at the wave vectors. The electron (hole) envelopes are calculated variationally by treating them as quasibound in an effective confinement region.[12] The envelope function $\Psi_{\alpha,\mathrm{env}}$ is an eigenfunction of the Hamiltonian

$$H_{ex} = \frac{\mathbf{p}_e^2}{2m_e} + V_e(z_e) + H_{\mathrm{LK}} + V_h(z_h) - \frac{e^2}{\varepsilon|\mathbf{r}_e-\mathbf{r}_h|}, \tag{2}$$

where $\mathbf{p}_e$ is the electron momentum operator, m_e is the electron effective mass (parabolic energy dispersion is assumed), $V_{e(h)}$ is the band-edge profile of the conduction (valence) band, H_{LK} is the 4×4 Luttinger-Kohn Hamiltonian for the hole, and the last term is the Coulomb interaction between the electron and the hole that is located at $\mathbf{r}_e$ and $\mathbf{r}_h$, respectively.

The equation for the expansion coefficients is obtained by multiplying the Schrödinger equation $H_{ex}\Psi_{\alpha,\mathrm{env}}=E_\alpha\Psi_{\alpha,\mathrm{env}}$ with the electron and hole envelope functions on the left followed by an integration in real space. In doing so, we assume that the light interacts with excitons at rest (i.e., the photon momentum is negligible) so that $F_{nm}^{\alpha}(\mathbf{k}_\parallel,\mathbf{q}_\parallel)=\delta(\mathbf{k}_\parallel+\mathbf{q}_\parallel)G_{nm}^{\alpha}(\mathbf{k}_\parallel)$ and apply the axial approximation to the hole state so that $g_m^{\nu}(z_h,\mathbf{k}_\parallel)=g_m^{\nu}(z_h,k_\parallel)e^{-i\nu\varphi}$. We also express the expansion coefficient $G_{nm}^{\alpha}(\mathbf{k}_\parallel)$ in terms of its magnitude and phase as $G_{nm}^{l\alpha}(k_\parallel)e^{il\varphi}$ (axial approximation decouples the excitons that have different l values[8]). The resulting equation for $G_{nm}^{\alpha}(\mathbf{k}_\parallel)$ becomes independent of the angle φ,

$$[E_n^e(k_\parallel)-E_m^h(k_\parallel)]G_{nm}^{l\alpha}(k_\parallel) + \sum_{n',m'}\sum_{\mathbf{k}_\parallel'} V_{nm,n'm'}^{l}(\mathbf{k}_\parallel,\mathbf{k}_\parallel')G_{n'm'}^{l\alpha}(k_\parallel') = E_{l\alpha}G_{nm}^{l\alpha}(k_\parallel), \tag{3}$$

except for the Coulomb interaction $V_{nm,n'm'}^{l}$,

$$V_{nm,n'm'}^{l}(k_\parallel,k_\parallel',\varphi') = \frac{-e^2}{\varepsilon q}\int\int dz_e dz_h f_{n'}^{*}(z_e) f_n(z_e) \times \sum_{\nu} g_{m'}^{\nu\,*}(k_\parallel',z_h) g_m^{\nu}(k_\parallel,z_h) e^{-q|z_e-z_h|} e^{i(l-\nu)\varphi'}, \tag{4}$$

where $q=\sqrt{k_\parallel^2+k_\parallel'^2-2k_\parallel k_\parallel'\cos\varphi'}$, φ' is the angle between $\mathbf{k}_\parallel$ and $\mathbf{k}_\parallel'$, $E_n^e(k_\parallel)-E_m^h(k_\parallel)$ is the joint energy dispersion of the nth electron and mth hole subbands, and $E_{l\alpha}$ is the eigenenergy of the $l\alpha$th state. The singularity arising along $\mathbf{k}_\parallel=\mathbf{k}_\parallel'$ in Eq. (4) can be eliminated by screening induced by the intrin-

sic carriers.[23] The envelope function for the exciton now becomes

$$\Psi^{l}_{\alpha,\mathrm{env}} = \sum_{n,m} \sum_{k_\parallel} G^{l\alpha}_{nm}(k_\parallel) f_n(z_e) \sum_{\nu} e^{i(l-\nu)(\theta-\pi/2)} g^{\nu}_{m}(z_h,k_\parallel) J_{l-\nu}(k_\parallel \rho), \tag{5}$$

where $J_{l-\nu}$ is the $(l-\nu)$th order Bessel function and ρ and θ are the magnitude and angle of the relative position vector $(\boldsymbol{\rho}_e - \boldsymbol{\rho}_h)$ of the exciton. In Eq. (5), the lth exciton state is the sum of four spinor components of the valence subbands and $(l-\nu)$ in the exponential term is the orbital angular momentum of the component ν. In the limit of the two-band model (one conduction- and one valence-subband state) and by assuming that the valence subbands do not mix strongly, we can safely define the two-dimensional orbital angular momentum quantum number of the lth exciton state as $m_l = l - \nu_m$ (analogous to the H atom: $m_l = 0, \pm 1, \pm 2, \ldots$ for s-, p-, d-like,… states, respectively) because the state is dominated by one of the four contributing components ν_m. For instance, the $e1$-$hh1$ exciton in an unbiased fairly narrow SQW is dominated by $\nu_m = \pm 3/2$ (for spin up and down) and $l = \nu_m$ and $l = \nu_m \pm 1$ for s-like $(m_l = 0)$ states and p-like $(m_l = \pm 1)$ states, respectively.[24] The variational approach is a convenient tool for solving Eq. (3), which is carried out by expanding $G^{l\alpha}_{nm}(k_\parallel)$ in a truncated set of Gaussian basis functions that minimizes the eigenenergy.[8] The oscillator strength is evaluated as

$$f^{l\alpha} = \frac{2}{m_0 E_{l\alpha}} \left| \sum_{\nu} \langle U_c | \boldsymbol{\varepsilon} \cdot \mathbf{p} | U_\nu \rangle \sum_{n,m,\mathbf{k}_\parallel} G^{l\alpha}_{nm}(k_\parallel) I^{\nu}_{nm}(k_\parallel) e^{i(l-\nu)\varphi} \right|^2, \tag{6}$$

where $\langle U_c | \boldsymbol{\varepsilon} \cdot \mathbf{p} | U_\nu \rangle$ is the bulk optical matrix between conduction band $|U_c\rangle$ and valence band $|U_\nu\rangle$ that depends on the polarization of the light $\boldsymbol{\varepsilon}$ and $I^{\nu}_{nm}(k_\parallel)$ is the $k_\parallel$-dependent overlap integral between conduction- and valence-subband envelope functions in the confined dimension. It is noted that even though the lth exciton state in Eq. (5) is composed of the four spinor components, only the single component that makes $l - \nu = 0$ in the exponential term contributes to the oscillator strength in Eq. (6).

B. Mixing of excitons originating in different subband pairs

We are focused on the mixing of the $e1$-$hh1$ and $e1$-$hh2$ excitons, where the major spinor component $(\nu_m = \pm 3/2)$ of the mixed exciton states remains the same as that of unmixed excitons obtained from the two-subband model, which retains m_l as a good quantum number even after the mixing. However, this is not always true for the mixing of heavy- and light-hole excitons; orbital angular momentum is not a good quantum number because the mixed state is not dominated by only one component.

Because p-like states have negligible oscillator strengths (unless they mix strongly to the s-like light-hole excitons and m_l is not well-defined anymore[6]), we consider the mixing of only s-like $(l = 3/2)$ states of $e1$-$hh1$ and $e1$-$hh2$ excitons in Eq. (3), which yields the 2×2 Hamiltonian matrix to be diagonalized,

$$H^{l} = \begin{bmatrix} T_{11} + V^{l}_{11,11} & V^{l}_{11,12} \\ (V^{l}_{11,12})^{*} & T_{12} + V^{l}_{12,12} \end{bmatrix}, \tag{7}$$

where T_{nm} is the kinetic energy of the nth electron and mth hole (to calculate p-like states, one only need change l to $1/2$). Neglecting exciton mixing is simply to set $V^{l}_{11,12} = 0$. Applying the variational approach to the diagonal element H^{l}_{11} (H^{l}_{22}) with an appropriate set of Gaussian basis functions and solving the matrix eigenvalue equation yields the energy $E^{l\alpha,UC}_{11(2)}$ and expansion coefficient $G^{l\alpha,UC}_{11(2)}(k_\parallel)$ of the uncoupled s-like ground- and excited-state excitons up to the number of the basis set. The degree of accuracy, however, decreases rapidly as the quantum number α of the excited state increases. When exciton mixing is considered, $V^{l}_{11,12}$ is no longer zero but must be computed, and the corresponding matrix eigenvalue equation yields the energy $E^{l\alpha,C}$ and the expansion coefficients

$$G^{l\alpha,C}(k_\parallel) = C_{11} G^{l\alpha,C}_{11}(k_\parallel) + C_{12} G^{l\alpha,C}_{12}(k_\parallel) \tag{8}$$

of the coupled excitons, where $C_{11(2)} G^{l\alpha,C}_{11(2)}(k_\parallel)$ is interpreted as the amplitude of the contribution of the $e1$-$hh1(2)$ subband pair to the coupled state $G^{l\alpha,C}(k_\parallel)$. Note that $G^{l\alpha,C}_{11(2)}(k_\parallel)$ is different from the uncoupled exciton state $G^{l\alpha,UC}_{11(2)}(k_\parallel)$.

C. Almost-degenerate perturbation theory

The mixed excitons can be calculated alternatively by applying almost-degenerate perturbation theory to the uncoupled states, which gives a convenient way to understand the physics of exciton mixing. The uncoupled states of the $e1$-$hh1$ and $e1$-$hh2$ excitons are evaluated as described above. The Coulomb interaction $V^{l}_{11,12}$ is then treated as a perturbation to the uncoupled states. The corresponding matrix to be diagonalized is

$$\begin{bmatrix} E^{l\alpha,UC}_{11} & V^{l}_{11,12} \\ (V^{l}_{11,12})^{*} & E^{l\alpha,UC}_{12} \end{bmatrix}, \tag{9}$$

where the Coulomb matrix element $V^{l}_{11,12}$ is evaluated by using the obtained uncoupled states:

$$V^{l\alpha\alpha'}_{11,12} = \sum_{\mathbf{k}_\parallel \mathbf{k}'_\parallel} G^{l\alpha',UC\,*}_{12}(k'_\parallel) V^{l}_{11,12}(k_\parallel, k'_\parallel, \varphi') G^{l\alpha,UC}_{11}(k_\parallel). \tag{10}$$

The corresponding mixed state is obtained as

$$G^{l\alpha}_{\mathrm{ADP}}(k_\parallel) = \sum_{\alpha'} [C_{l\alpha,11} G^{l\alpha',UC}_{11}(k_\parallel) + C_{l\alpha,12} G^{l\alpha',UC}_{12}(k_\parallel)], \tag{11}$$

where the coefficients $C_{l\alpha,11(2)}$ are the components of the eigenvectors obtained from the diagonalization, which are the portions of the contribution of the uncoupled states to the mixed ones. Note that Eqs. (8) and (11) are not the same.

III. RESULTS AND DISCUSSION

We first analyze two ADQWs having different degrees of coupling in the anticrossing bias range and show that the

f-sum rule breaks down dramatically if exciton mixing is neglected. This is followed by a detailed investigation of the excitonic-mixing effect on the oscillator strengths and energy levels. We also discuss that the almost-degenerate perturbation theory can be misleading if carelessly applied.

A. Effect of exciton mixing in strongly and weakly coupled ADQWs

The effects of $e1$-$hh1$ and $e1$-$hh2$ exciton mixing in an anticrossing bias range are investigated in two ADQW samples, ADQW-30 and ADQW-12, which consist of 3 and 1.2 nm thick $Al_{0.25}Ga_{0.75}As$ coupling barriers, respectively, and two GaAs wells (widths ~6.5 and ~3.5 nm). The mole fraction of the confining walls is the same as that of the coupling barrier. The material parameters are adopted from Ref. 8.

The mixing is strong in ADQW-30 because the energy difference between the ground states of the $e1$-$hh1$ and $e1$-$hh2$ excitons becomes much smaller than the exciton binding energy in this sample, as shown in Fig. 1(a). The energy differences between the band-to-band transitions (dotted) and the coupled lowest two excitons (solid) can be interpreted as the exciton ground-state binding energies. As stated in Ref. 14, the band-to-band transition energies (energy difference between the electron and the hole subbands at $k_{\|}=0$) anticross at much lower bias (~25 kV/cm) than those of the coupled excitons do (~31 kV/cm), both very sharply over very narrow bias ranges due to the thick coupling barrier. The binding energies, however, are exchanged gradually from ~25 to ~31 kV/cm. This implies that severe mixing of excitons as well as VBM between the $hh1$ and $hh2$ subbands occur in this bias range. In Fig. 1(a), the uncoupled exciton energies (dashed), however, do not even anticross, showing the change of the binding energy at the anticrossing bias of the band-to-band transitions due to the neglect of the mixing effect, which is incorrect.

The corresponding oscillator strengths of the uncoupled and coupled states are shown in Figs. 1(b) and 1(c). The transfer of oscillator strength from the $e1$-$hh1$ to the $e1$-$hh2$ ground-state excitons occurs around ~25 and ~31 kV/cm in the uncoupled and coupled cases, respectively. Moreover, the sum of the oscillator strengths of the two uncoupled states [dashed curves in Fig. 1(b)] is not uniform in the anticrossing bias range, while this is not so in the coupled case. (The reason for the breakdown of the *f*-sum rule in the uncoupled case will be discussed later in this section.) The minimum of the sum of the oscillator strengths in the uncoupled case at 25.3 kV/cm is only 45% of the summed value outside the anticrossing range as shown in Fig. 1(b).

Figure 1(d) shows that the oscillator strength $f^{1s,C}$ of the coupled ground state has a major contribution from the $e1$-$hh1$ (dotted with marks) subband pair until the bias reaches ~25 kV/cm following which the $e1$-$hh2$ (dotted) subband pair contribute the majority, which maintains $f^{1s,C}$ uniform until the bias reaches just below ~31 kV/cm [$f_{11}^{1s,C}$ and $f_{12}^{1s,C}$ are obtained from Eq. (6) by taking the modulus square of $nm=11$ and $nm=12$ separately instead of summing up in advance, which is not physically measurable; this is

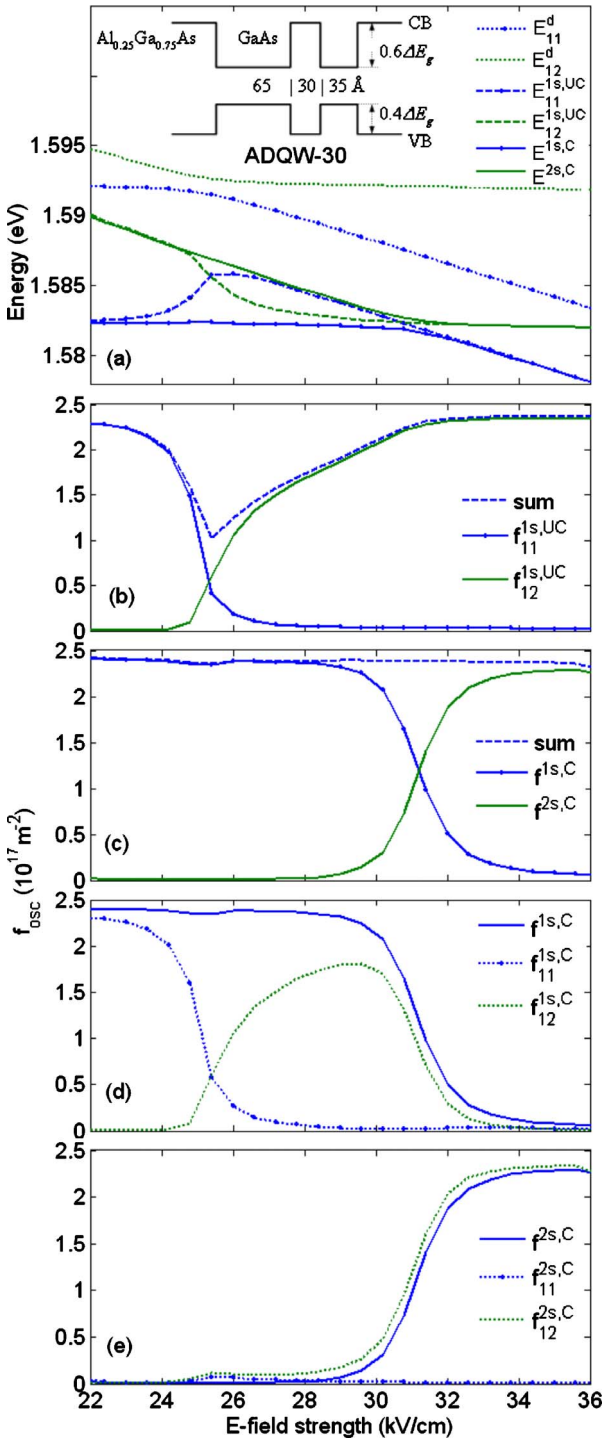

FIG. 1. (Color online) Energy levels and oscillator strengths of excitons in ADQW-30 as a function of the bias field strength. The inset in (a) is the band-edge diagram along the growth direction. (a) Energy levels (solid: coupled excitons $E^{\alpha s,C}$, dashed: uncoupled ground-state excitons $E_{11(2)}^{1s,UC}$, and dotted: band-to-band transitions $E_{11(2)}^{d}$; $e1$-$hh1$ excitons have dots on the curves). Oscillator strengths of (b) uncoupled ground states $f_{11(2)}^{1s,UC}$ and (c) coupled ground- and excited-state excitons $f^{\alpha s,C}$ (solid) and their sums (dashed). Oscillator strengths of the coupled (d) ground- and (e) first excited-state excitons (solid) and the contributions from $e1$-$hh1$ (dotted with marks, $f_{11}^{\alpha s,C}$) and $e1$-$hh2$ (dotted, $f_{12}^{\alpha s,C}$) subband pairs.

adopted only to show the portion of the contribution of each subband pair to the coupled states]. Figure 1(e) shows that the oscillator strength of the $e1$-$hh2$ ground-state exciton may be slightly overestimated when only $f_{12}^{2s,C}$ is accounted for [the sum of the contributions from the two subband pairs ($e1$-$hh1$ and $e1$-$hh2$) in the modulus square of Eq. (6) is smaller than that of only the $e1$-$hh2$ subband pair].

The mixing effect is expected to be weak in ADQW-12 because the minimum difference of the band-to-band transition energies in the anticrossing bias range is ~7 meV, which is almost the same as the binding energies of the uncoupled ground-state excitons at the same bias ~33 kV/cm, as shown in Fig. 2(a). The energy differences before (dashed) and after (solid) the inclusion of coupling are less than 1 meV in both $e1$-$hh1$ and $e1$-$hh2$ ground-state excitons. The minimum of the sum of the oscillator strengths in the uncoupled case, however, is only 66% of the expected value [Fig. 2(b)], which is substantial, while the f-sum rule is conserved in the coupled case as shown in Fig. 2(c). This shows that weak coupling in terms of the energy level can still have a substantial effect on the oscillator strength. In Fig. 2(c), the oscillator strength of the first excited state is transferred to the higher excited states sequentially as the bias increases, which is due to the coupling of the uncoupled $e1$-$hh1$ excited states and the $e1$-$hh2$ ground state.

B. Analysis in $k_\parallel$ space

The mixing of excitons is attributed to the Coulomb interaction of the excitons, which appears in the off-diagonal element in Eq. (7). In the following, we discuss the effect of this term on the exciton envelope functions and the corresponding oscillator strengths. We pick a bias field of ~26 kV/cm in an ADQW-30 that exhibits strong excitonic mixing.

The valence subband dispersion is plotted in Fig. 3(a), where the $hh1$ and $hh2$ subbands are seen to anticross at ~0.15 nm^{-1} (vertical dotted line). Figure 3(b) shows the Coulomb matrix elements as functions of $k_\parallel$ that are obtained from Eq. (4) by taking the integral along φ' and putting $k'_\parallel = 0$, which shows the approximate trend of the $k_\parallel$-dependent Coulomb interaction [in the calculation, the full two-dimensional $(\mathbf{k}_\parallel, \mathbf{k}'_\parallel)$-dependence should be considered]. The diagonal elements $(V_{11,11}, V_{12,12})$ have their largest values near $k_\parallel = 0$ and decrease gradually until the two subbands anticross following which they decrease more rapidly and fall to zero. Thus the resulting $k_\parallel$-dependent $G_{11}^{1s,UC}$ for the uncoupled ground-state exciton originating in the $e1$-$hh1$ subband pair, for example, has very little contribution after the anticrossing $k_\parallel$ value, as shown in Fig. 3(c). This leads to the negligible oscillator strength integrand $GI_{11}^{1s,UC}$ in the corresponding $k_\parallel$ range [solid line in Fig. 3(d)], where $GI_{nm}^{l\alpha}$ represents the integrand $G_{nm}^{l\alpha}(k_\parallel) I_{nm}^{\nu}(k_\parallel)$ in Eq. (6). On the other hand, the off-diagonal element $V_{11,12}$ that represents the Coulomb interaction between the $e1$-$hh1$ and $e1$-$hh2$ subband pairs begins to increase from zero at $k_\parallel = 0$ and reaches its maximum at the value of $k_\parallel$ near the anticrossing, which exceeds $V_{11,11}$ in this sample at the given bias field. This means that the Coulomb coupling of the $e1$-$hh2$ to the

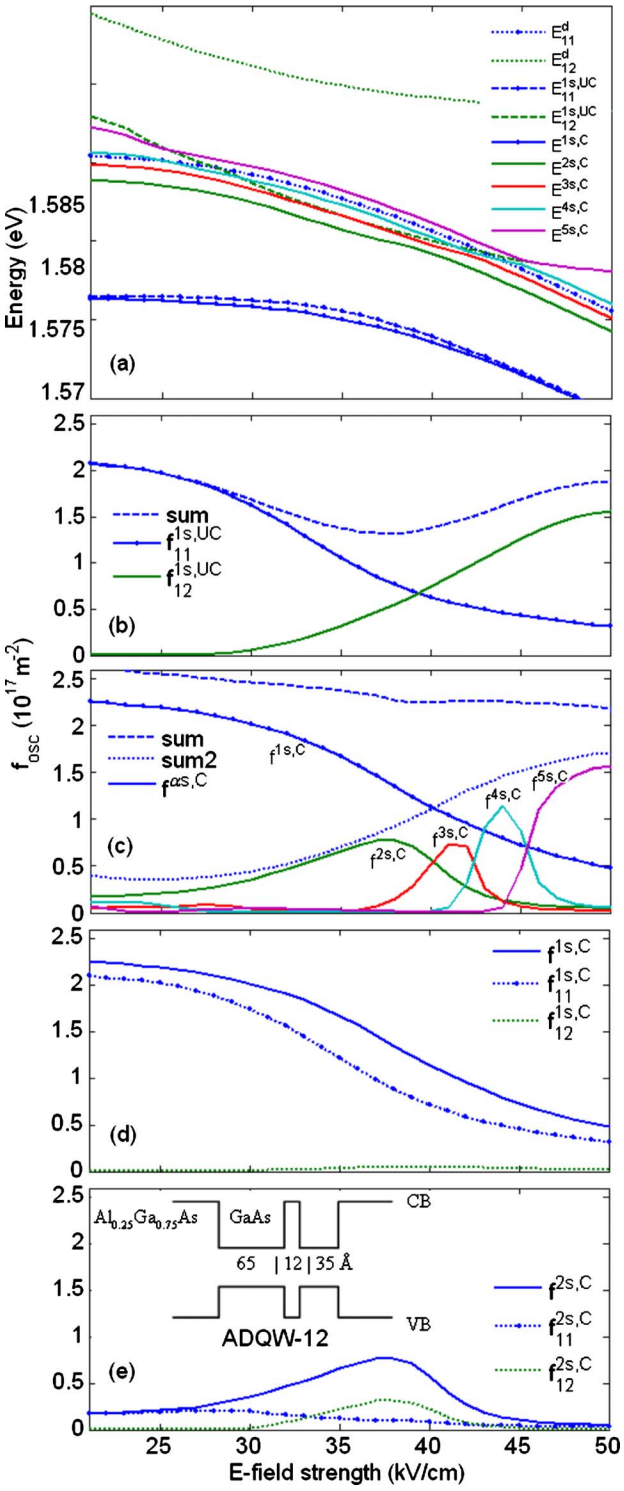

FIG. 2. (Color online) Energy levels and oscillator strengths of excitons in ADQW-12 as a function of the bias field strength. (a) Energy levels of excitons (solids from the lowest to highest: from ground to fourth coupled excitons $E^{\alpha s,C}$, lower dashed: $E_{11}^{1s,UC}$, upper dashed: $E_{12}^{1s,UC}$). Oscillator strengths of (b) uncoupled ground-state excitons $f_{11(2)}^{1s,UC}$ (solid) and their sum (dashed) and (c) coupled excitons $f^{\alpha s,C}$ up to fourth excited states (solid) and their sum (dashed: total sum and dotted: sum except $f^{1s,C}$, which shows the sequential transfer of oscillator strength to higher state). (d) and (e) are the same as those of Fig. 1.

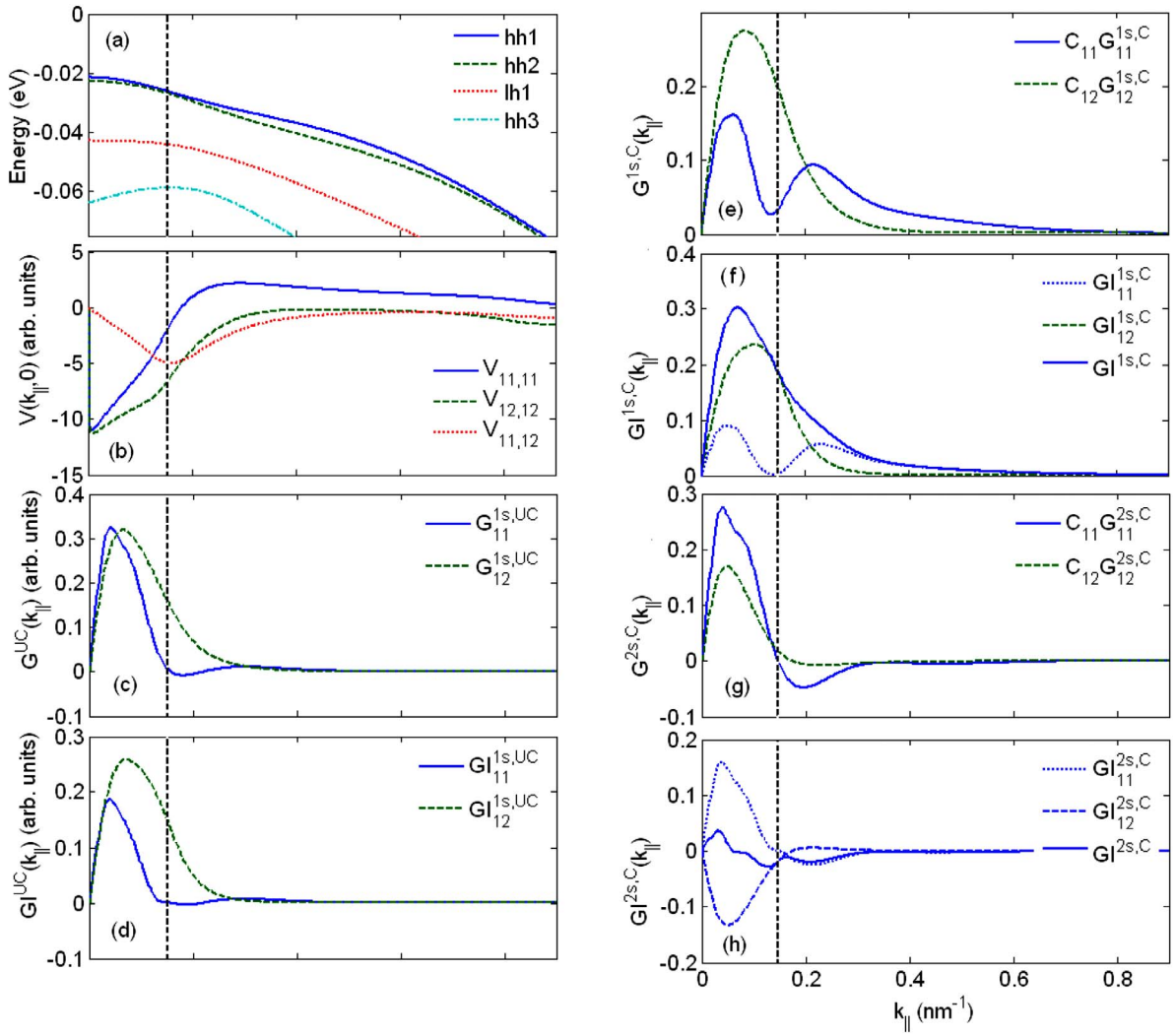

FIG. 3. (Color online) (a) Energy dispersions of four highest valence subbands, (b) one-dimensional diagonal and off-diagonal Coulomb matrix elements, (c) expansion coefficients of uncoupled ground-state excitons, (d) integrands of oscillator strengths of uncoupled ground-state excitons in Eq. (6), (e) components of coupled ground-state excitons in Eq. (8), (f) the corresponding integrands of oscillator strengths (dotted and dashed) and their sum (solid), (g) components of coupled first excited-state exciton in Eq. (8), and (h) the corresponding integrands of oscillator strengths (dotted and dashed) and their sum (solid) as a function of the in-plane wave vector in ADQW-30 at the bias field of ~26 kV/cm. The vertical dotted line indicates the wave vector where *hh*1 and *hh*2 subbands anticross.

$e1$-$hh1$ subband pair is larger than the Coulomb interaction between the $e1$ and $hh1$ subbands. As a result of the coupling, the lowest exciton expansion coefficients $G^{1s,C}$ is expressed as a mixture of the basis $G_{11}^{1s,C}$ and $G_{12}^{1s,C}$ whose $k_\parallel$-dependent profiles significantly differ from the uncoupled expansion coefficients $G_{nm}^{1s,UC}$. The basis $G_{11(2)}^{1s,C}$ for the coupled state in Fig. 3(e) retains substantial values even after the anticrossing $k_\parallel$ while $G_{nm}^{1s,UC}$ in Fig. 3(c) does not. Consequently, the overall value of $GI^{1s,C}$ of the ground state for the coupled case in Fig. 3(f) that is obtained by adding $GI_{11}^{1s,C}$ and $GI_{12}^{1s,C}$ has a significantly larger contribution than the sum of the uncoupled ones [$GI_{11}^{1s,UC}$ and $GI_{12}^{1s,UC}$ in Fig. 3(c)] after the anticrossing $k_\parallel$ value. By following the same procedure, the coupled first excited state $G^{2s,C}$ that corresponds to the uncoupled $e1$-$hh2$ ground-state exciton is found to have negligible oscillator strength as shown in Fig. 3(h).

In summary, neglecting the Coulomb coupling between different subband pairs in a sample that exhibits strong VBM results in diminishing the contribution of the $k_\parallel$-dependent subband pairs after the anticrossing $k_\parallel$ value, which leads in turn to the underestimation of the oscillator strength, breaking the f-sum rule.

C. Almost-degenerate perturbation theory

Almost-degenerate perturbation theory was applied to the uncoupled states of ADQW-30 to account for the mixing of excitons. In this case, the mixed states are expressed as a linear combination of the uncoupled states as in Eq. (11). Employing the two uncoupled ground states $G_{11}^{1s,UC}$ and $G_{12}^{1s,UC}$ only as a basis set for the purpose of obtaining the coupled ground and first excited states, however, did not yield accurate energy levels or oscillator strengths, as shown in Figs. 4(a) and 4(b); the sum of the oscillator strengths is exactly the same as that of the uncoupled ground states due to the unitarity of the transformation to diagonalize the per-

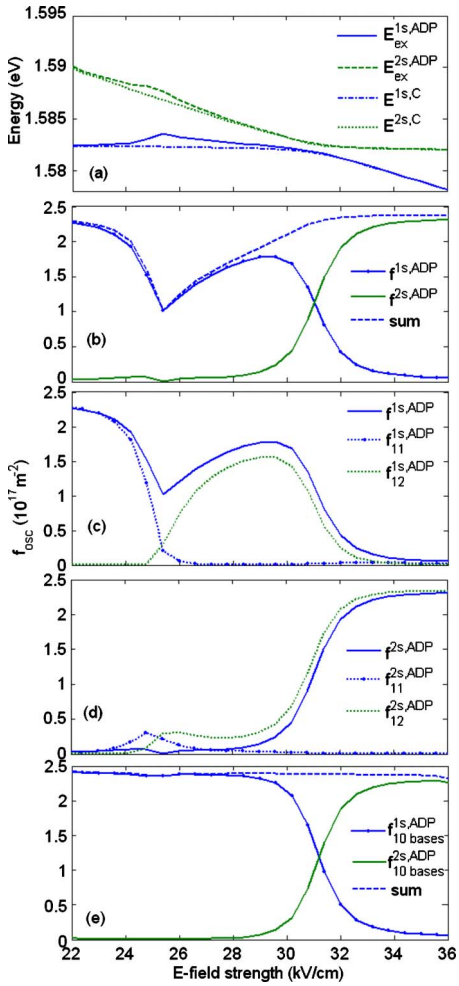

FIG. 4. (Color online) Bias-dependent energy levels and oscillator strengths of excitons of ADQW-30 that are obtained by applying the almost-degenerate perturbation (ADP) theory. (a) Energy levels of excitons obtained by ADP with two bases $E_{ex}^{\alpha s,\mathrm{ADP}}$ that show notable deviation from $E^{\alpha s,C}$. Oscillator strengths of coupled excitons (solid) from ADP with (b) two bases and (e) ten bases and their sum (dashed). Oscillator strengths of the coupled (c) ground-state and (d) first excited-state excitons from ADP with two bases (solid) and the contributions to it from $e1$-$hh1$ (dotted with marks) and $e1$-$hh2$ (dotted) subband pairs.

turbation matrix (see the Appendix). It is found that incorporating only the *ground states* of the uncoupled excitons obtained including VBM as a basis set is insufficient to account accurately for the strongly mixed exciton states [however, neglecting the VBM (i.e., constant effective mass) and incorporating the uncoupled ground states may yield valid results[13,14]]. The same results as those obtained from the full mixing model were obtained by incorporating up to ten excited uncoupled states as shown in Fig. 4(e). The results in Figs. 4(c) and 4(d), obtained by using only two ground states, however, show that in the bias range from ~25 to ~31 kV/cm the majority of the oscillator strength in the lowest exciton state is attributed to the uncoupled upper ground-state exciton $G_{12}^{1s,UC}$ as a result of strong mixing between the two uncoupled ground-state excitons caused by the Coulomb interaction.

IV. SUMMARY

The mixing effect of excitons originating in different subband pairs in ADQWs was investigated in the range of electric field where the two highest heavy-hole subbands mix strongly in their dispersions. In this bias range, neglecting the Coulomb interaction between the two subband pairs in the inclusion of the valence band mixing effect introduces significant error in both the energy levels and the oscillator strengths of the corresponding excitons when the middle barrier is thick. Even in ADQW-12 where the middle barrier is relatively thin and the energy difference between the uncoupled and the coupled excitons is smaller than 1 meV, the sum of the oscillator strengths was only ~66% of the correct value. This implies that neglecting the mixing of excitons at the anticrossing in designing optical devices that utilizes ADQW structures is logically inconsistent and can lead to invalid estimates of device performances. Detailed wave-vector-dependent analysis of the Coulomb matrix elements and the expansion coefficients revealed the reason for the breakdown of the f-sum rule when the mixing effect was ignored: neglecting the Coulomb coupling between different subband pairs results in diminishing the contribution of the $k_{\|}$-dependent subband pairs after the anticrossing $k_{\|}$ value, which leads to the underestimation of the oscillator strength. In addition, it was found that applying almost-degenerate perturbation theory to the uncoupled ground-state excitons for the purpose of including the mixing effect can also lead to erroneous results due to the insufficient number of basis functions.

ACKNOWLEDGMENTS

The authors would like to thank Stephen Hughes of Queens University for fruitful discussions. This work was supported in part by the National Science Foundation by Grants ECCS-0523923 and NSF DMR-0305524.

APPENDIX

The oscillator strengths of the uncoupled ground-state excitons $f_{11(2)}^{1s,UC}$ are calculated from Eq. (6) as

$$f_{11(2)}^{1s,UC} \sim |GI_{11(2)}^{1s,UC}|^2, \tag{A1}$$

and their sum $f_{\mathrm{sum}}^{1s,UC}$ is

$$f_{\mathrm{sum}}^{1s,UC} = f_{11}^{1s,UC} + f_{12}^{1s,UC} \sim |GI_{11}^{1s,UC}|^2 + |GI_{12}^{1s,UC}|^2. \tag{A2}$$

The application of the almost-degenerate perturbation theory to the two uncoupled ground states yields two mixed states

$$G_{\mathrm{ADP}}^{1s,C} = c_1 G_{11}^{1s,UC} + c_2 G_{12}^{1s,UC}$$

and

$$G_{\mathrm{ADP}}^{2s,C} = c_2 G_{11}^{1s,UC} - c_1 G_{12}^{1s,UC}, \tag{A3}$$

where c_1 and c_2 are the elements of the eigenvectors that are obtained by diagonalizing Eq. (9), which are normalized $(c_1^2+c_2^2=1)$. From Eq. (6), the corresponding oscillator strengths are

$$f_{1s,\mathrm{ADP}} \sim |c_1 GI_{11}^{1s,UC} + c_2 GI_{12}^{1s,UC}|^2$$

and

$$f_{2s,\mathrm{ADP}} \sim |c_2 GI_{11}^{1s,UC} - c_1 GI_{12}^{1s,UC}|^2. \tag{A4}$$

Adding $f^{1s,\mathrm{ADP}}$ and $f^{2s,\mathrm{ADP}}$ after taking the modulus square yields the same expression as $f_{\mathrm{sum}}^{1s,UC}$ in Eq. (A2).

*Electronic address: dkkim@gatech.edu

[1] E. E. Mendez, G. Bastard, L. L. Chang, L. Esaki, H. Morkoc, and R. Fischer, Phys. Rev. B **26**, 7101 (1982).
[2] D. A. B. Miller, D. S. Chemla, T. C. Damen, A. C. Gossard, W. Wiegmann, T. H. Wood, and C. A. Burrus, Phys. Rev. Lett. **53**, 2173 (1984).
[3] G. Bastard, E. E. Mendez, L. L. Chang, and L. Esaki, Phys. Rev. B **28**, 3241 (1983).
[4] T. H. Wood, C. A. Burrus, D. A. B. Miller, D. S. Chemla, T. C. Damen, A. C. Gossard, and W. Wiegmann, Appl. Phys. Lett. **44**, 16 (1984).
[5] G. D. Sanders and K. K. Bajaj, Phys. Rev. B **35**, 2308 (1987).
[6] L. Viña, R. T. Collins, E. E. Mendez, and W. I. Wang, Phys. Rev. Lett. **58**, 832 (1987).
[7] G. E. W. Bauer and T. Ando, Phys. Rev. B **38**, 6015 (1988).
[8] L. C. Andreani and A. Pasquarello, Phys. Rev. B **42**, 8928 (1990).
[9] S. Jorda, U. Rössler, and D. Broido, Phys. Rev. B **48**, 1669 (1993).
[10] R. Winkler, Phys. Rev. B **51**, 14395 (1995).
[11] S. R. Andrews, C. M. Murray, R. A. Davies, and T. M. Kerr, Phys. Rev. B **37**, 8198 (1988).
[12] J. Lee, M. O. Vassell, E. S. Koteles, and B. Elman, Phys. Rev. B **39**, 10133 (1989).
[13] T. Kamizato and M. Matsuura, Phys. Rev. B **40**, 8378 (1989).
[14] A. M. Fox, D. A. B. Miller, G. Livescu, J. E. Cunningham, and W. Y. Jan, Phys. Rev. B **44**, 6231 (1991).
[15] W. Chen and T. G. Andersson, Semicond. Sci. Technol. **7**, 828 (1992).
[16] M. M. Dignam and J. E. Sipe, Phys. Rev. B **43**, 4084 (1991).
[17] J. Soubusta, R. Grill, P. Hlídek, M. Zvára, L. Smrčka, S. Malzer, W. Geißelbrecht, and G. H. Döhler, Phys. Rev. B **60**, 7740 (1999).
[18] P. Steinmann, B. Borchert, and B. Stegmüller, IEEE Photonics Technol. Lett. **2**, 191 (1997).
[19] M. Aguilar, M. Carrascosa, F. Agullo-Lopez, F. Agullo-Rueda, M. R. Melloch, and D. D. Nolte, J. Appl. Phys. **86**, 3822 (1999).
[20] X. Chen, W. Batty, M. P. Earnshaw, D. W. E. Allsopp, and R. Grey, IEEE J. Quantum Electron. **34**, 1180 (1998).
[21] M. Y. Su, S. G. Carter, M. S. Sherwin, A. Huntington, and L. A. Coldren, Phys. Rev. B **67**, 125307 (2003).
[22] S. Ristic and N. A. F. Jeager, IEEE Photonics Technol. Lett. **18**, 316 (2006).
[23] S. Hughes, Phys. Rev. B **69**, 205308 (2004).
[24] References 8–10 discuss this topic in detail.